Stem Cell Research & Therapy

RESEARCH

Open Access

LncRNA MRF targeting FSHR inhibits the osteogenic differentiation of BMSCs and bone defect repair through the regulation of the cAMP-PKA-CREB signaling pathway

Qing Ning[1], Ming Li[1], Zhuangyao Liao[1], Enming Chen[1], Huatao Liu[1], Yuwei Liang[1], Yuanquan Chen[1], Yuxi Li[1*] and Lin Huang[1*]

Abstract

Background Mesenchymal stem cells (MSCs), known for their ability to differentiate into osteoblasts, play a pivotal role in bone metabolism. In our previous investigations, we identified a novel long non-coding RNA (lncRNA) named MCP1 Regulatory Factor (MRF), which exhibits significant involvement in immune regulation of BMSCs. Moreover, we observed noticeable expression changes of MRF during the osteogenic differentiation of BMSCs. However, the exact role and underlying mechanism of MRF in the osteogenic differentiation of BMSCs remain elusive.

Methods QRT-PCR analysis was employed to assess the expression levels of MRF. RNA interference and overexpression plasmids were utilized to modulate MRF expression, allowing for the observation of changes in the osteogenic differentiation capacity of BMSCs. Downstream pathways involved in the MRF-mediated regulation of BMSCs' osteogenic differentiation were predicted using transcriptome sequencing. The functionality of MRF in vivo was validated through a mouse tibial drilling defect model.

Results In patients with osteoporosis, there is a notable increase in the expression of MRF within BMSCs. During the osteogenic differentiation of BMSCs, the MRF expression progressively decreases. The knockdown of MRF significantly enhances the osteogenic differentiation of BMSCs, promoting an increased expression of bone-related proteins such as RUNX2, ALP, and COL1A1. Transcriptome sequencing and western blot indicated that cAMP/PKA/CREB signaling pathway was significantly activated after lncRNA-MRF knockdown. Moreover, in the mouse tibial drilling defect model, MRF knockdown significantly promotes ossification in vivo.

Conclusions MRF modulates the cAMP/PKA/CREB signaling pathway via the follicle stimulating hormone receptor (FSHR), thereby influencing the ossification differentiation of BMSCs. Our research suggests that MRF may serve as a potential target for bone-related disorders.

Keywords LncRNA, BMSCs, Osteogenesis, MRF, FSHR

[†]Qing Ning and Ming Li have contributed equally to this work.

Lin Huang: Lead contact

*Correspondence:
Yuxi Li
liyx73@mail.sysu.edu.cn
Lin Huang
huangl5@mail.sysu.edu.cn
[1] Department of Orthopedics, Sun Yat-Sen Memorial Hospital, Sun Yat-Sen University, Guangzhou 510120, People's Republic of China

Introduction

MSCs are extensively researched and considered promising for bone regeneration and repair [1]. Bone marrow mesenchymal stem cells (BMSCs) are a vital source of osteoblasts with the potential for multi-directional differentiation. The process of osteogenic differentiation in BMSCs is precisely regulated to maintain skeletal health, but abnormalities in this differentiation can result in conditions like osteoporosis, skeletal deformities, and delayed fracture healing. Although numerous factors regulate the osteogenic differentiation of BMSCs, the precise mechanism remains largely unknown.

Long non-coding RNA (lncRNA) represent a distinct class of RNA molecules, defined by their lengths exceeding 200 nucleotides and their inability to encode proteins, or their capacity to encode only small peptides [2]. These molecules interact with DNA, RNA, and proteins, playing vital regulatory roles in various biological pathways like cellular metabolism, the cell cycle, tumor invasion, and metastasis. Studies have demonstrated that lncRNA also influence bone formation by modulating the growth and differentiation of osteoblasts and osteoclasts. A recent study by Zhang et al. [3] revealed that lncRNA Nron is critical for osteoclast differentiation, as it regulates the nuclear translocation of NFATc1. In addition to their tri-lineage differentiation capacity, BMSCs also exhibit significant immunomodulatory capabilities, which are integral to their overall function [4]. In our initial research focusing on how mononuclear cells impact BMSCs [5], we analyzed the gene expression of BMSCs co-cultured with mononuclear cells compared to those cultured in isolation. This analysis led to the discovery of a significant lncRNA named lncRNA MRF that be crucial for the immunoregulatory function of BMSCs. Considering the substantial changes in MSC behavior induced by mononuclear cells through lncRNA MRF and the known influence of osteoclasts on MSC osteogenic differentiation, we hypothesize that lncRNA MRF may play a pivotal role in the osteogenic differentiation process of BMSCs.

In our initial investigation, we conducted a proteomics analysis on the binding proteins of lncRNA MRF, demonstrating its role in modulating the immunomodulatory functions of BMSCs via the HNRNPD-MCP1 axis [5]. Specifically, MRF upregulates the expression of monocyte chemoattractant protein 1 (MCP-1), thereby enhancing the recruitment of monocytes. Inhibiting MRF expression enhances the ability of MSCs to suppress M1 macrophage polarization and promote M2 polarization. However, the comprehensive changes in downstream genes and regulatory pathways involved in the osteoblastic differentiation of BMSCs mediated by lncRNA MRF are still not fully understood. The differentiation of BMSCs can be influenced by various mechanisms, with numerous studies focusing on lncRNA-mediated cell differentiation. For example, Coralee E. Tye et al. [6] conducted a transcriptome analysis on hMSCs induced for osteogenic differentiation over 0, 7, and 14 days, revealing a decrease in the expression of lncRNA (MIR181A1HG) during ossification. Silencing this lncRNA in MSCs enhanced differentiation towards osteo-chondroprogenitors, resulting in changes in expression and BMP2 responsiveness of skeletal gene networks such as SOX5 and DLX5. Wang et al. [7] identified a novel lncRNA-IUR associated with Bcr-Abl-mediated cellular transformation using gene-chip technology. They highlighted its role as a critical negative regulator of Bcr-Abl-induced tumorigenesis. Knocking down lncRNA-IUR significantly increased the survival of Abl-transformed leukemia cells in mice and promoted tumor growth. Through RNA-seq analysis, they found that lncRNA-IUR suppresses Bcr-Abl-mediated tumor formation by inhibiting CD71 expression regulated by STAT5. Transcriptome sequencing is commonly employed to investigate regulatory mechanisms. Differential analysis tools, such as Gene Ontology (GO) and Kyoto Encyclopedia of Genes and Genomes (KEGG), applied to post-transcription sequencing data, facilitate the identification of downstream regulatory molecules associated with lncRNA.

Our research revealed a negative correlation between lncRNA MRF and the osteogenic differentiation of BMSCs, showing that lncRNA MRF can suppress the osteogenic differentiation capacity of BMSCs. Through transcriptional sequencing and Western blot analysis, we found that lncRNA MRF regulates BMSCs' osteogenic differentiation via the FSHR/cAMP/PKA/CREB signaling pathway. Furthermore, in a mouse bone defect model, inhibiting lncRNA MRF was shown to enhance bone healing. These results provide additional evidence on the functional role of lncRNA MRF in BMSCs and represent the first study showing a lncRNA that concurrently regulates BMSCs differentiation and immune modulation.

Materials and methods

BMSCs isolation and culture

Bone marrow tissue was aseptically collected from patients undergoing spinal surgery at the Department of Orthopedics, Sun Yat-sen Memorial Hospital, between October 2021 and May 2024. Inclusion criteria: 1) Patients with intervertebral disc degeneration who have surgical indications. Exclusion criteria: 1) Pregnant or lactating women; 2) Individuals with psychiatric disorders who cannot provide informed consent; 3) Patients with spinal tuberculosis, spinal infections, or other infectious diseases; 4) Patients with ankylosing spondylitis

or other spinal diseases; 5) Patients with spinal tumors. Except for the BMSCs from normal and osteoporotic patients used in Fig. 1c, subsequent experiments were conducted using BMSCs from patients without osteoporosis. All included osteoporotic patients were newly diagnosed and had not received anti-osteoporosis treatment at the time of surgery. Following the addition of Hydroxyethyl Starch separation solution, BMSCs were isolated and purified using density gradient centrifugation. The experimental procedures involved BMSCs from the second to fifth generation. Cells were cultured in a medium consisting of 90% Dulbecco's Modified Eagle's Medium (DMEM, Gibco, New York, USA) with 1 g/L D-Glucose and 10% Fetal Bovine Serum (FBS, TIANHANG, Zhejiang, China). The culture bottles were placed in an incubator set at 37 degrees Celsius with 5% carbon dioxide and 20% oxygen. The medium was changed every two days until the cells reached 80–90% confluence.

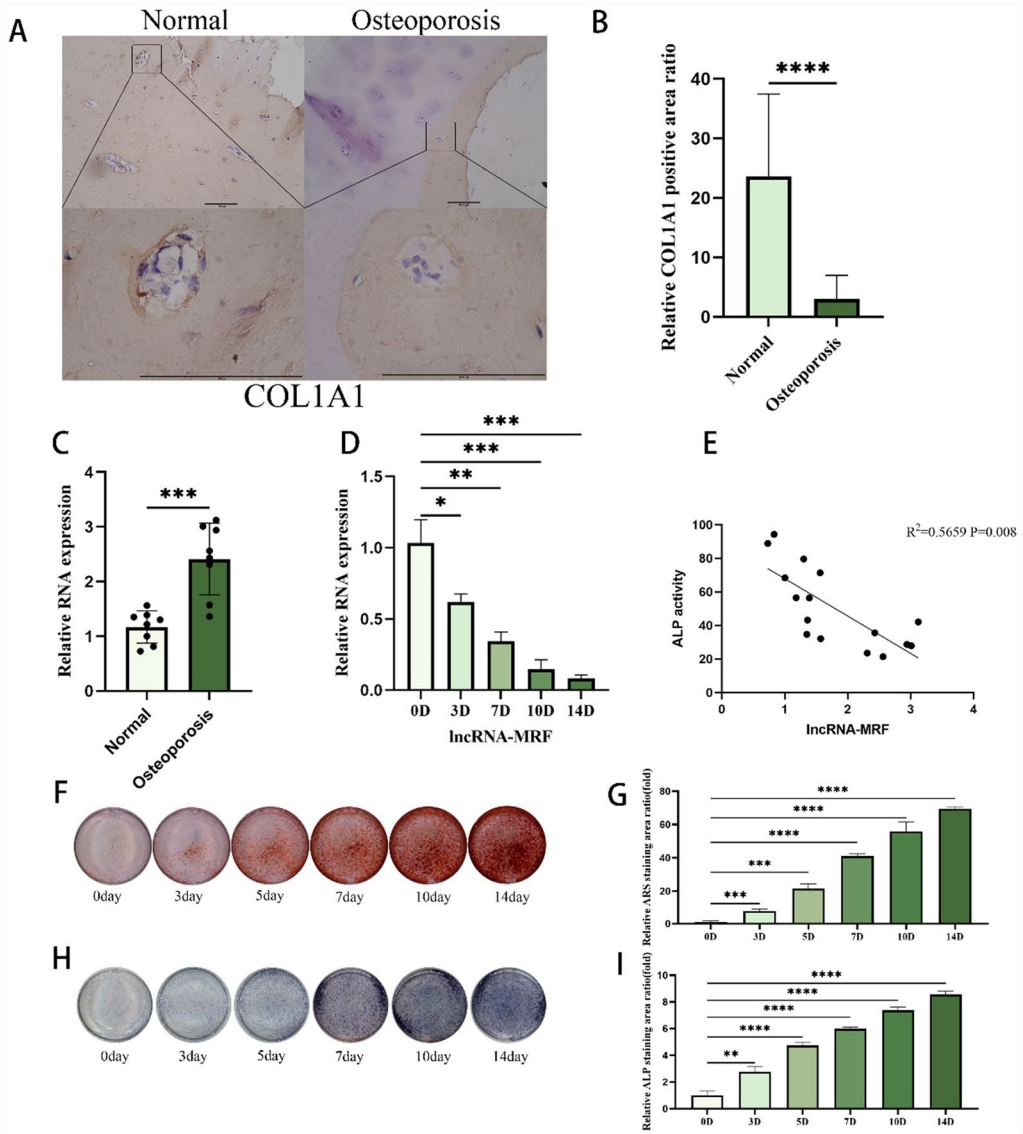

Fig. 1 LncRNA MRF are elevated in osteoporosis, showing a negative correlation with osteoblast differentiation. **a** Immunohistochemistry of Col1A1 in normal bone tissue and bone tissue of patients with osteoporosis. **b** The positive area ratio was evaluated by Image J(n = 3). **C** Comparison of LncRNA MRF in BMSCs between normal and osteoporotic patients using qPCR (n = 8). **d** QPCR detection of changes in LncRNA MRF in BMSCs induced by time gradient osteogenesis (n = 3). **e** Correlation analysis between LncRNA MRF and ALP activity (n = 16). **f** ARS staining after time gradient induced osteogenic differentiation of BMSCs. **g** Image J was used to analyze the positive area of ARS staining (n = 3) **h** ALP staining after time gradient induced osteogenic differentiation of BMSCs. **i** Image J was used to analyze the positive area of ALP staining(n = 3), The data are presented as the mean ± SD (*p <0.05, **p <0.01, ***p < 0.001)

RNA interference and Plasmid construction and transfection

After reaching 80% confluence, third-generation BMSCs underwent transfection with lncRNA MRF specific siRNA, synthesized by GenePharma (Shanghai), or FSHR-specific siRNA, synthesized by IGE Biotechnology (Guangzhou), as outlined in Table 1. The transfection process involved the use of Opti-mem and Lipofectamine 3000 Transfection Reagent (Thermo Fisher Scientific, Waltham, MA, USA) following the manufacturer's instructions. This method introduced targeted MRF (SI-MRF) siRNA, targeted FSHR (SI-FSHR) siRNA and non-targeted control siRNA (NC) (GenePharma, Shanghai) into the BMSCs. Additionally, to induce MRF overexpression, the MRF plasmid was created by gene create (Wuhan, China) and transfected into the BMSCs using the pcDNA3.1 vector and Lipofectamine 3000 Transfection Reagent. Subsequently, the BMSCs were either collected for interference efficiency measurement after 72 h or used in other experiments.

Osteogenic differentiation

The third-generation BMSCs are digested, resuspended, and seeded at a density of $5*10^5$ cells/well in a 6-well plate. Osteogenic induction is carried out using a medium consisting of 10% Fetal Bovine Serum (FBS), 50 μg/mL of ascorbic acid, 10 mmol/L of β-glycerophosphate, and 0.1 mM of dexamethasone in 90% Dulbecco's Modified Eagle Medium (DMEM) with 1 g/L of D-Glucose. The cells are then placed in an incubator at 37 °C and 5% CO2, with the osteogenic medium replaced every two days until the BMSCs are ready for further experimentation.

ARS staining assay

BMSCs were fixed in a 4% paraformaldehyde solution for 15 min, then treated with 500 μl of 1% Alizarin Red S (ARS) in a 24-well plate. After 15 min, the staining solution was removed, and the plate was washed thrice with phosphate-buffered saline (PBS). The results were analyzed by scanning the plate with an imaging scanner and quantifying using Image J.

ALP assay

The BMSCs were fixed in a 4% paraformaldehyde solution for 15 min and then subjected to ALP staining using the BCIP/NBT ALP reagent kit (Beyotime, China) according to the manufacturer's instructions. The stained cells were observed under an optical microscope, and quantitative analysis of the results was carried out using Image J software.

Quantitative real-time polymerase chain reaction

The EZB reagent (MA, USA) was used as instructed by the manufacturer to isolate total RNA from BMSCs. Subsequently, the Prime Script RT Master Mix was employed for reverse transcription, involving an incubation at 37 °C for 15 min followed by denaturation at 85 °C for 5 s to synthesize complementary DNA (cDNA) from the extracted RNA. RT-PCR was conducted using SYBR Premix Ex Taq, and relative gene expression was determined using GAPDH as a reference gene. The expression of the target gene mRNA was assessed using the ΔΔCT method, with primer details available in Table 2.

Western blot

After adding protease inhibitor (1%) and phosphatase inhibitor (1%) (Cwbio, Jiangsu, China) to RIPA buffer for lysis, the solution was added to the BMSCs samples. Following a 30-min incubation for protein digestion by protease, the mixture was centrifuged to extract total protein. Each sample, containing 20 μg of protein, underwent protein immunoblot analysis. The pre-boiled protein samples were loaded with SDS-PAGE Loading Buffer onto a 4%-20% SDS-PAGE gel (ACE Biotechnology) and electrophoresed at 145 V for 50 min. The gel was transferred to a PVDF membrane (Millipore, Billerica, MA, USA) at 400 mA for 65 min. After membrane blocking for 1 h with 5% BSA in TBST solution, it was incubated overnight at 4 °C with specific primary antibodies. These included antibodies from IMMNOWAY (anti-CREB, anti-P-CREB, anti-FSHR), PROTEINTECH (anti-ALP, anti-RUNX2, anti-COL1A1), Santa Cruz (anti-PKA, anti-P-PKA), Cwbio (anti-GAPDH), and Bioworld (anti-β-ACTIN). Following three washes with TBST, the membrane was incubated with the secondary antibody for 1 h, followed by three additional washes with TBST. Finally, light signals were captured using an ECL imaging

Table 1 Specific siRNA sequences of lncRNA MRF and FSHR

Gene name	Sense (5′–3′)	Antisense (5′–3′)
lncRNA MRF-homo-294	GGGACACAUUUAUUGAUGUTT	ACAUCAAUAAAUGUGUCCCTT
lncRNA MRF-homo-389	GUGGAUGAAACAUCAAUAUTT	AUAUUGAUGUUUCAUCCACTT
FSHR-1	GGUCGACUUACAACUUAAAtt	UUUAAGUUGUAAGUCGACCtt

Table 2 RT-PCR primer sequences

Primer name	Sequence (5′–3′)
lncrnaF	TGCCCACTACCTCATTCCCA
lncrnaR	TGGAGTGGAGACTGTTCCGT
RUNX2-F	TGTCATGGCGGGTAACGAT
RUNX2-R	AAGACGGTTATGGTCAAGGTGAA
ALP-F	CCACGTCTTCACATTTGGTG
ALP-R	AGACTGCGCCTGGTAGTTGT
OCN-F	TTCTTTCCTCTTCCCCTTG
OCN-R	CCTCTTCTGGAGTTTATTTGG
hhipf	AATGCAGAGCCACGGTACAA
hhipr	GCTGGCTCACATTTTGCAGT
ATP2B2f	TGGTGATTTTCATAGCCAAGAGC
ATP2B2r	GTGAGCTCCAAGAGGTGTCC
CALM3f	GAGGGAAAGTAGTCCGGCG
CALM3r	GTCAGCTGGTCAGCCTACG
VAV1f	GCCGACATGGGCAAGATTTC
VAV1r	GGCCTGCTGATGGTTCTCTT
PPARAf	TGTGGCAAGACAAGCTCAGA
PPARAr	GTGAAAGCGTGTCCGTGATG
fshr-f	GCTTTGAAAGTGTGTGTCTCTATGGC
fshr-r	CAGAGGCTCCGTGGAAAACA
GAPDH-F	ACAGTTGCCATGTAGACC
GAPDH-R	TTTTTGGTTGAGCACAGG
OPN-F	ACTCGAACGACTCTGATGATGT
OPN-R	GTCAGGTCTGCGAAACTTCTTA

system (Syngene G:BOX ChemiXT 4, United Kingdom) for final analysis. Quantitative analysis of the results was performed using Image J.

Immunofluorescence

Cells were washed three times with PBS, followed by fixation in 4% paraformaldehyde. Subsequently, three additional washes with PBS were performed, followed by permeabilization with 0.5% Triton X-100 for 5 min. After three more rinses with PBS, the cells were blocked with 10% bovine serum albumin at 37 °C in a humid chamber for one hour. Following this, primary antibodies against COL1A1 (1:200) and P-PKA (1:200) were applied overnight at 4 °C in the dark. After the primary antibody incubation, cells were washed with PBS and then incubated with the secondary antibody (Alexa Fluor® 488, 1:100) at 37 °C for one hour. Subsequent to three rounds of PBS washing, a 1-min DAPI staining was performed. Fluorescence images were captured using an Olympus BX 63 microscope (New York, USA), and the results were quantified using Image J for fluorescence analysis.

Histological and immunohistochemical staining

Tissue specimens were fixed in 4% formaldehyde for 48 h, decalcified for more than 30 days, and then embedded in paraffin and made slices. Following the manufacturer's protocols, histological sections were stained with Hematoxylin and Eosin, as well as Safranin O-Fast Green and tartrate-resistant acid phosphatase (TRAP) staining, to assess the extent of defect repair. Immunohistochemistry involved incubating tissues with primary antibodies targeting COL1A1 (1:200) and p-CREB (phosphorylated-cAMP-responsive element binding protein) (1:200) overnight, followed by the application of secondary antibodies to murine tibial defect specimens. Photomicrographs were captured using a NIKON NI-U microscope, and quantitative image analysis was conducted using Image J. Antibodies were sourced from Proteintech (USA) and Immunoway (Plano, USA).

Micro- CT

Micro-computed tomography (micro-CT) is utilized to examine the tibial bone structure in this study. Mice are euthanized using an intraperitoneal injection of pentobarbital at a dose of 50 mg/kg. The tibial tissue is then fixed in 4% paraformaldehyde for 48 h and stored at 4℃ in 70% ethanol. The micro-CT scan and image acquisition are carried out by the Department of Nuclear Medicine at the Animal Center of Sun Yat-sen University. Analysis of bone volume/total volume (BV/TV), trabecular thickness, trabecular number, and trabecular separation is performed following established guidelines. Two-dimensional and three-dimensional images of the bone structure are reconstructed from the obtained slices.

Transcriptome sequencing

Utilizing RNA-seq technology, we investigated the gene expression profile during osteoblast differentiation following the knockdown of MRF. When the cultures reached 80% confluence in 75 cm^2 culture bottles, BMSCs were transduced using Opti-mem and Lipofectamine 3000 Transfection Reagent (Thermo Fisher Scientific, Waltham, MA, USA) as per the manufacturer's instructions, with siRNA targeting MRF (SI-MRF) and negative control siRNA (NC) (GenePharma, Shanghai). Subsequently, osteogenesis induction was carried out for three days. A total of six cell samples from the NC1/SI1, NC2/SI2, and NC3/SI3 groups were analyzed. These samples were obtained from a 16-year-old female, a 30-year-old male, and a 69-year-old male, all of whom did not have osteoporosis. In the RNA-Seq experiment, each sample was individually cultured using second-generation BMSCs. The cell concentration reached (10^6) cells/ml, and all samples passed the company's quality inspection.

BMSCs from different patients were not mixed. Total RNA was extracted from the BMSCs using TRIzol reagent (BASMDTSCI). Transcriptional sequencing of the samples was conducted by Xu ran biological (Shanghai, China), In order to identify differentially expressed genes between different sample groups using DESeq2 software, the differential expression range can be filtered by satisfying the criteria of $|\log2FC| \geq 1$ and p value ≤ 0.05 to select the differentially expressed genes between two groups. For the analysis of differential expression gene dataset, the TopGO software was used to conduct functional analysis of Gene Ontology (GO). Additionally, KEGG pathway enrichment analysis was performed using the Metascape database.

Surgical procedures

The animal experiments conducted at Sun Yat-Sen University were approved by the SYSU Institutional Animal Care and Use Committee (SYSU-IACUC-2024-001134). C57BL/6 mice (12 weeks, 18–22 g) were obtained from the Shuiyuntian Biology Company (Guangzhou, China). The left and right tibias of each mouse were assigned to different groups and drill holes separately, with one group treated with a blank siRNA and the other with a lncRNA MRF knockdown siRNA. A total of 12 mice were used in the study. The mice were anesthetized with isoflurane, and their lower limbs were prepared for surgery by sterilization. Following a small skin incision and muscle isolation to expose the tibia, a 0.8 mm diameter hole was drilled at a suitable location. The lncRNA MRF knockdown siRNA (5 nmol; 10 μL) or negative control siRNA was then introduced into the hole. The muscles were repositioned, and the skin was sutured and disinfected. The lncRNA MRF knockdown siRNA was administered every two days following the surgery. At 1 and 2 weeks after surgery, mice were euthanized by intraperitoneal injection of 1% pentobarbital sodium under excessive anesthesia (100 mg/kg) and their tibia was extracted for subsequent experiments. Throughout the study, the mice were housed in a pathogen-free environment with access to food and water, and were maintained on a 12-h light/dark cycle in a temperature-controlled room [8].

Dual-luciferase reporter assay

The promoter sequence of the FSHR was synthesized and subsequently cloned into the pGL3-Basic vector by IGE Biotechnology (Guangzhou). Utilizing Lipofectamine 3000 (Thermo Fisher Scientific, Waltham, MA, USA), the aforementioned vector was transfected into 293 T cells. Following transfection, the cells were subjected to either siRNA treatment to silence lncRNA MRF or were transfected with an overexpression plasmid to enhance lncRNA MRF expression. In all experimental conditions, cells were additionally co-transfected with the pRL-TK plasmid to serve as an internal control. The luciferase activity was then measured using the Dual-Luciferase Reporter Assay System (APExBIO, USA). Relative luciferase activity was evaluated in accordance with the manufacturer's guidelines.

Cell counting kit-8 assay

We inoculated 96-well plates with 2×10^3 cells per well and allowed them to adhere for 24 h. Following this, we added varying concentrations of H-89 (1, 5, 10, 20, 40, 80, and 160 μM) dissolved in DMSO, sourced from Selleck (United States). After treatment with H-89, we added a medium containing 10% CCK-8 solution to each well and incubated the plates at 37 °C for 1 h. The absorbance was then measured at 450 nm using an enzyme labeler.

Statement

The work has been reported in line with the ARRIVE guidelines 2.0.

Statistical analysis

Each experiment was repeated a minimum of three times, and the results were presented as the mean ± standard deviation. Statistical analysis was performed using GraphPad Prism 9 software (La Jolla, CA, USA). The Student' s t-test and two-way ANOVA were utilized to determine statistical significance, with p values less than 0.05 deemed as statistically significant.

Results

LncRNA MRF are elevated in osteoporosis, showing a negative correlation with osteoblast differentiation.

In the preliminary phase, we have established the length and pertinent information of lncRNA MRF. Its entire length was found to be 1531 bp, located on the short arm of chromosome 12. Simultaneously, we gathered bone specimens from three patients with osteoporosis and three patients who underwent spinal surgery for scoliosis. Immunohistochemical staining for COL1A1 [9] confirmed a decrease in bone formation markers in osteoporosis patients [10] (Fig. 1a, b). To further explore the influence of lncRNA MRF on BMSCs, we utilized BMSCs from eight patients with osteoporosis and eight control patients with hip dysplasia but without osteoporosis. Following RNA extraction, qPCR analyses were conducted, revealing an upregulation of lncRNA MRF expression in BMSCs derived from osteoporosis patients (Fig. 1c). Considering the significant role of BMSCs in the occurrence and progression of osteoporosis, we investigated the changing trends of lncRNA MRF expression during BMSCs osteogenic differentiation. The results demonstrated a progressive decline in lncRNA MRF levels

concomitant with increasing induction of osteogenesis, as demonstrated by ARS and ALP staining, as well as ALP detection and qPCR analyses (Fig. 1d, f, h, g, i). Moreover, lncRNA MRF exhibited an inverse correlation with alkaline phosphatase activity (Fig. 1e). These findings suggest a strong association between lncRNA MRF expression and bone metabolism in osteoporosis. Collectively, these results indicate that lncRNA MRF may serve as a negative regulator during BMSCs osteogenic differentiation and bone formation.

The knockdown and overexpression of LncRNA MRF influence the osteogenic differentiation of BMSCs.

In order to investigate the role of lncRNA MRF in the osteogenic differentiation of BMSCs, we constructed and selected two siRNAs with relatively high knockdown efficiency for lncRNA MRF (shRNA-1 and shRNA-2) (Table 1). The results from ARS and ALP experiments (Fig. 2a, b) indicate an enhanced differentiation of BMSCs into osteoblasts upon the reduction of lncRNA MRF expression. Following the transfection with OE-MRF, both ARS staining and ALP assays (Fig. 2d, e) indicated a marked decrease in the osteogenic differentiation of BMSCs. qPCR data revealed a similar upward trend in the mRNA levels of osteogenic markers ALP, RUNX2, OCN, and OPN following the suppression of lncRNA MRF expression (Fig. 2c). In the group subjected to over-expression of lncRNA MRF (OE-MRF), there was a significant elevation in the expression level of lncRNA MRF in the BMSCs. Correspondingly, the mRNA levels showed a decline in osteogenic activity, with decreased expression of ALP, RUNX2, OCN, and OPN (Fig. 2f). Western blot analysis confirmed these observations, showing that a decrease in lncRNA MRF expression led to an increase in osteogenic markers, including ALP, RUNX2, and COL1A1 proteins, while lncRNA MRF overexpression exhibited the reverse trend (Fig. 2g, h, i, j). Immunofluorescence data also support these findings, as evidenced by the notable rise in the fluorescence intensity of COL1A1, after a reduction in lncRNA MRF expression (Fig. 2k, l). After over-expressing lncRNA MRF, the fluorescence intensity of COL1A1 had substantially reduced (Fig. 2m, n). The above experiments indicate that lncRNA MRF has an inhibitory effect on the osteogenic differentiation regulation of BMSCs.

Targeting lncRNA MRF holds the potential to enhance bone formation in vivo.

To further investigate the role of lncRNA MRF in osteogenesis in vivo, we conducted an animal experiment with a drilled-hole model (Fig. 3a). After drilling holes near the epiphysis of the mouse tibia with a 0.8 mm drill bit, we administered injections of SI-MRF or negative controls (Fig. 3b). Following treatment with either negative controls siRNA or lncRNA MRF knockdown siRNA for seven or fourteen days, we utilized micro-CT scanning to assess the damage site. Both external and internal general vistas of the femur revealed a relatively deficient cortical bone covering in the siRNA blank control injection group, while the lncRNA MRF knockdown siRNA group demonstrated a more substantial bone filling of deficits, suggesting an accelerated healing rate (Fig. 3c). In the lncRNA MRF knockdown siRNA injection group, we have observed a pronounced increase in the BV/TV ratio and Trabecular Thickness (Fig. 3d, e, f, g) as well as a significantly higher Trabecular Number within the callus tissue (Fig. 3h, j) and less Trabecular Spacing (Fig. 3i, k). The bone defect healing rate in the lncRNA MRF knockdown siRNA group was also higher than that in the control group (Fig. 3l, m). This suggests that lncRNA MRF knockdown siRNA can effectively enhance bone repair in the context of mouse tibia deficiencies. H&E staining (Fig. 3n) and Safranin O/Fast Green (Fig. 3o) staining show a more continuous cortical bone and more trabecular connections at the site of tibia-drilled hole deficiencies in the lncRNA MRF knockdown siRNA injection group. To investigate whether LncRNA-MRF affects other cells involved in bone formation within the bone

(See figure on next page.)

Fig. 2 The knockdown and overexpression of LncRNA MRF influence the osteogenic differentiation of BMSCs. a Treatment of BMSCs with shRNA-1 and shRNA-2 during osteogenic differentiation followed by ARS/ALP staining. **b** Image J was used to analyze the positive area of ARS/ALP staining (n = 3). **c** qPCR detection of mRNA expression of osteogenic related molecules after knock-down of LncRNA MRF (n = 3). **d** Treatment of BMSCs with MRF overexpression plasmid during osteogenic differentiation followed by ARS/ALP staining. **e** Image J was used to analyze the positive area of ARS/ALP staining (n = 3). **f** qPCR detection of mRNA expression of osteogenic related molecules after overexpression of LncRNA MRF (n = 3). **g**, **i** Western blot showing changes in the expression of osteogenic related proteins after knocking down or overexpressing LncRNA MRF. **h**, **j** Quantification of specific signal intensities. GAPDH was used as the loading control. Values are presented as mean ± standard deviation (SD) for three independent experiments (n = 3) *p <0.05, **p <0.01, ***p <0.001. *k*, **l**, **m** Immunofluorescence images (20 X) showing COL1A1 staining of BMSCs treated shRNA-1, shRNA-2, and MRF overexpression plasmids and Osteogenic induction for three days. **n** Image J was used to analyze the Immunofluorescence intensity of COL1A1 (n = 3). The data are presented as the mean ± SD (*$p < 0.05$, **$p < 0.01$, ***$p < 0.001$)). Full-length blots are presented in Supplementary material 1: Figures 1–8, The cropping position of the original image is marked in Supplementary material 1: documents 1

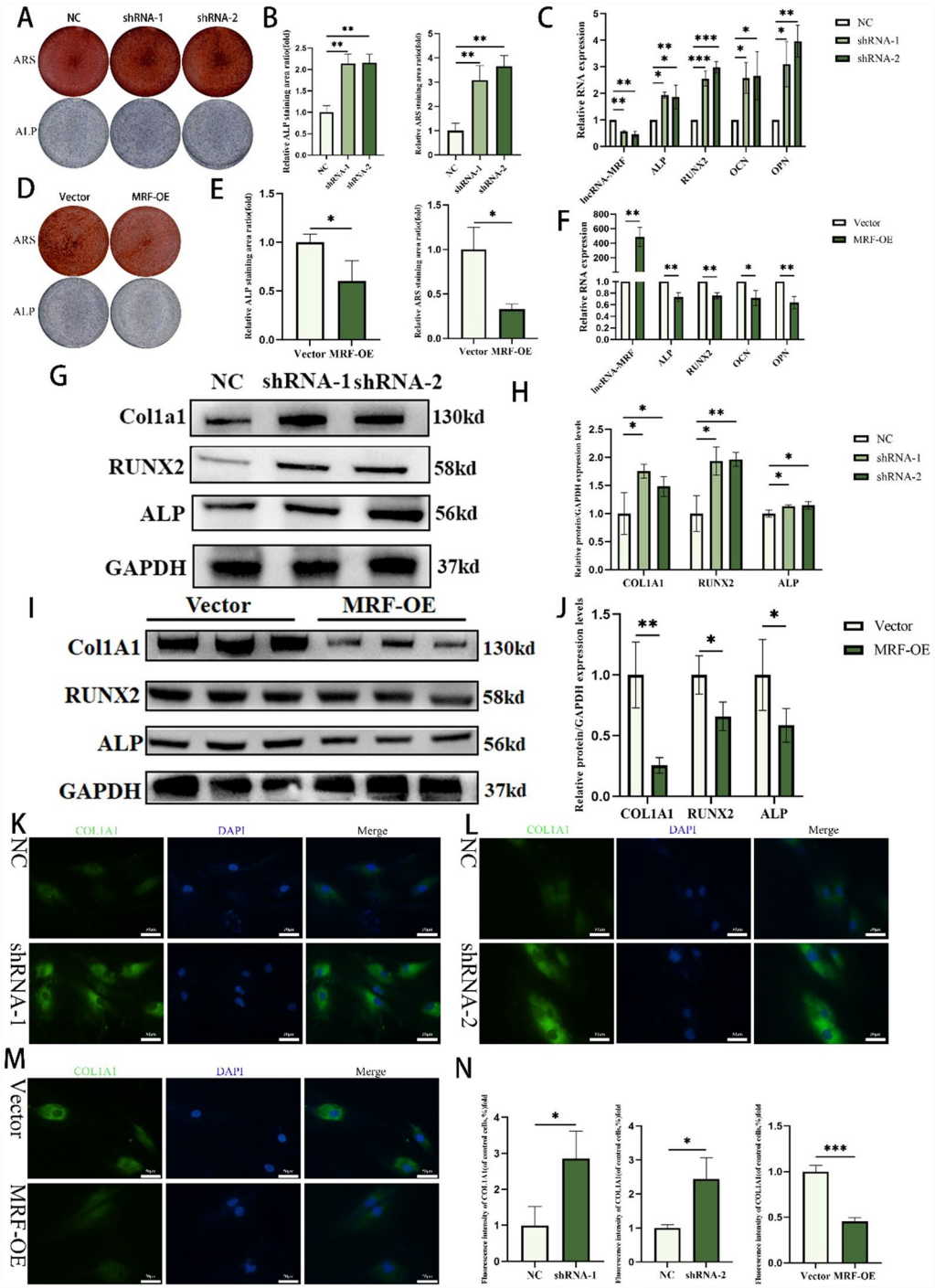

Fig. 2 (See legend on previous page.)

microenvironment, such as osteoclasts, we performed TRAP staining on tissue sections from the drilled areas (Fig. 3p, q). The results showed no significant difference in the number of osteoclasts between tibias injected with SI-MRF and those injected with negative controls (Fig. 3r). This indicates that SI-MRF does not primarily exert its effects through osteoclasts. Immunohistochemistry reveals a larger number of COL1A1-positive cells (Fig. 3s, t, u). The above results indicate that inhibiting lncRNA MRF in vivo has a promoting effect on bone repair.

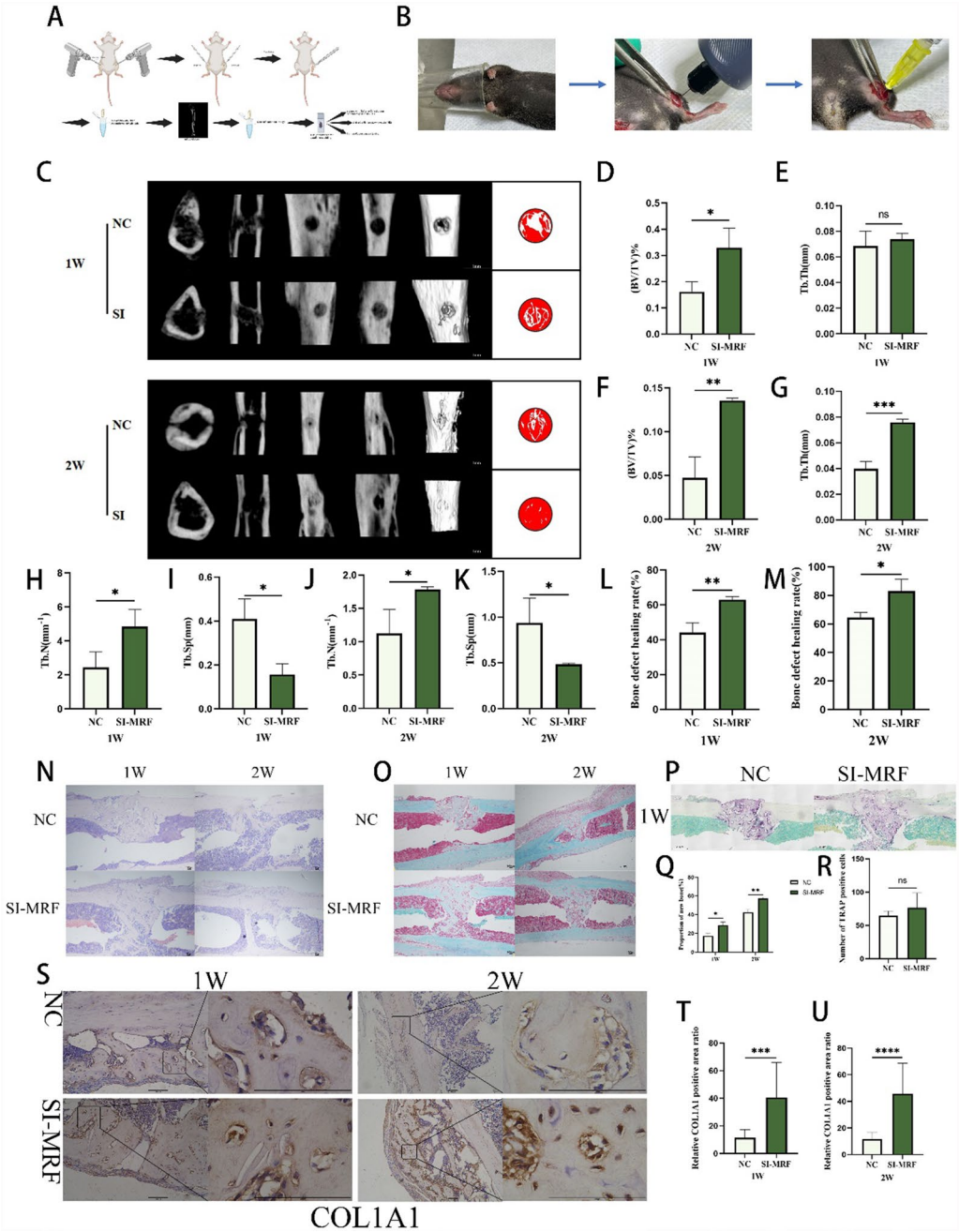

Fig. 3 Targeting lncRNA-MRF holds the potential to enhance bone formation in vivo. **a** Overall flowchart of animal experiments. **b** Picture of Mouse Surgical Process. **c** In vivo micro-CT demonstrated , at 1w and 2w, local injection of negative controls siRNA or lncRNA MRF knockdown siRNA displayed in bone repair at the site of drilling injury, and the group injected with lncRNA MRF knockdown siRNA showed better bone repair The new generating bone formed part of the drill-hole area was indicated with red mark. **d-k** The following parameters were calculated when analyzing the bone repair situation at the damaged area of the drill-hole: bone volume per total volume (BV/TV), Trabecular Thickness (Tb. Th), Trabecular Number (Tb. N), Trabecular Spacing (Tb. Sp). **l**, **m** Image J was used to analyze the bone defect healing rate, The data are presented as the mean ± SD (*$p < 0.05$, **$p < 0.01$, ***$p < 0.001$). **n**, **o** Histological analysis including HE and Safranin O and Fast Green staining showed the degree of local bone repair after injection of negative controls siRNA or lncRNA MRF knockdown siRNA. **p** osteoclast staining showed the number of osteoclasts after injection of negative controls or lncRNA MRF knockdown siRNA. **q** Image J was used to analyze the proportion of new bone, The data are presented as the mean ± SD (*$p < 0.05$, **$p < 0.01$, ***$p < 0.001$). **r** The number of osteoclasts was calculated using image j. **s** Immunohistochemistry of Col1A1 in local injection of negative controls siRNA group or lncRNA MRF knockdown siRNA group with 1w or 2w. **t**, **u** The positive area ratio was evaluated by Image J. The data are presented as the mean ± SD (*$p < 0.05$, **$p < 0.01$, ***$p < 0.001$). Six mice were used in 1W group and 2W group respectively, n = 6

DGE was analyzed before and after silencing LncRNA MRF using RNA-seq technology.

To provide further clarity on the mechanism underlying the regulation of osteogenic differentiation of BMSCs by lncRNA MRF, we conducted RNA-seq to identify differentially expressed genes (DEGs) before and after lncRNA MRF knockdown. The results revealed expression changes in 384 genes (Fig. 4a), with 201 genes showing increased expression, and 183 genes showing decreased expression (Fig. 4b). Functional enrichment analysis of DEGs using Gene Ontology (GO) revealed insights into Biological Process, Cell Component, and Molecular Function (Fig. 4c). We have identified the ten most prominent upregulated and downregulated genes (Fig. 4d), the analysis of which will bolster our understanding and verification of DEGs. The chord plot illustrated GO function enrichment (Fig. 4e), while the scatter plot demonstrated the relationship between Pathways and DEGs based on KEGG pathway classification (Fig. 4f). The analysis revealed significant enrichment in pathways such as Galactose Metabolism, Pentose Phosphate Pathway, B Cell Receptor Signaling Pathway, and cAMP Signaling Pathway. Notably, six genes were enriched in the cAMP signaling pathway, which showed a high degree of enrichment and a strong correlation with osteogenic differentiation. To validate the RNA-seq findings, we conducted PCR verification on the molecules enriched in the cAMP signaling pathway (Fig. 4j). The cAMP signaling pathway is an important and classic pathway that affects the osteogenic differentiation of BMSCs, and its upstream can be regulated by G-protein coupled receptors. Our RNA-seq results showed a significant upregulation of FSHR (Fig. 4g), alongside notable enrichment of the cAMP signaling pathway. It is speculated that FSHR, as a G-protein coupled receptor, may regulate the osteogenic differentiation of MSCs by affecting the downstream cAMP signaling pathway. Therefore, we conducted validations. Western blot results (Fig. 4h, l) demonstrated that the reduction of lncRNA MRF in BMSCs leads to increased FSHR protein expression and a simultaneous rise in FSHR mRNA levels (Fig. 4k). The cAMP signaling pathway mainly functions through the phosphorylation of PKA and downstream effector molecules, so we assessed the phosphorylation ratios of PKA and CREB following the knockdown or overexpression of lncRNA MRF. A significant increase in the ratios of p-PKA and p-CREB was observed (Fig. 4i, m, n). The results support the hypothesis that the osteogenic-inducing activity of lncRNA MRF may be associated with the cAMP metabolic pathway [11].

The LncRNA MRF governs osteogenic differentiation via the FSHR-cAMP-PKA-CREB signaling pathway.

To investigate the specific mechanisms by which LncRNA-MRF regulates FSHR and to determine whether LncRNA-MRF influences the cAMP/PKA/CREB signaling pathway via FSHR mediation, we constructed a luciferase reporter plasmid containing the FSHR promoter and performed dual-luciferase assays. The findings revealed that compared to the NC group, 293 T cells treated with SI-MRF exhibited increased luciferase activity. Conversely, overexpression of LncRNA MRF resulted in a significant decrease in luciferase activity within 293 T cells (Fig. 5b). This result suggests that LncRNA MRF may inhibit the transcription of FSHR, indicating that the regulation of FSHR mRNA by LncRNA MRF occurs through modulation of its transcriptional activity (Fig. 5a). We also designed specific siRNA for the knockdown of FSHR (SI-FSHR) and conducted rescue experiments. The results indicated that following treatment with SI-MRF, BMSCs showed a significant increase in the ratios of P-PKA/PKA and P-CREB/CREB, suggesting substantial activation of the cAMP-PKA-CREB signaling pathway. Subsequently, we performed concurrent knockdown of FSHR alongside MRF. The results demonstrated that BMSCs subjected to the simultaneous knockdown

(See figure on next page.)

Fig. 4 DGE was analyzed before and after silencing LncRNA MRF using RNA-seq technology. **a** For the differentially expressed genes screened between sample groups, bidirectional hierarchical clustering of genes and samples was performed and displayed using a heatmap. **b** Volcanic diagram of DGE between two sample groups. **c** Functional enrichment analysis of DEGs using Gene Ontology (GO) revealed insights into Biological Process, Cell Component, and Molecular Function. **d** the ten most prominent upregulated and downregulated genes. **e** The chord plot of GO function enrichment. **f** the scatter plot about the relationship between Pathways and DEGs based on KEGG pathway classification. **g** The expression changes of FSHR in the volcano map of RNA sequencing results. **h** Western blot showing changes in the expression of FSHR after knocking down or overexpressing LncRNA MRF. **i** Western blot showing changes in the expression of P-PKA/PKA, P-CREB/CREB after knocking down or overexpressing LncRNA MRF. **j** The molecules enriched in the cAMP signaling pathway were confirmed using PCR, the data are presented as the mean ± SD (*$p < 0.05$, **$p < 0.01$, ***$p < 0.001$) (n = 3). **k** Changes in mRNA expression of FSHR after knocking down LncRNA MRF (n = 3). **l** Quantification of specific signal intensities. GAPDH was used as the loading control. Values are presented as mean ± standard deviation (SD) for three independent experiments (*$p < 0.05$, **$p < 0.01$, ***$p < 0.001$) (n = 3). **m**, **n** Quantification of specific signal intensities. GAPDH was used as the loading control. Values are presented as mean ± standard deviation (SD) for three independent experiments (n = 3) (*$p < 0.05$, **$p < 0.01$, ***$p < 0.001$). A total of six cell samples from the NC1/SI1, NC2/SI2, and NC3/SI3 groups were analyzed. n = 3. Full-length blots are presented in Supplementary material 1: Figure 9–24, The cropping position of the original image is marked in Supplementary material 1: documents 1

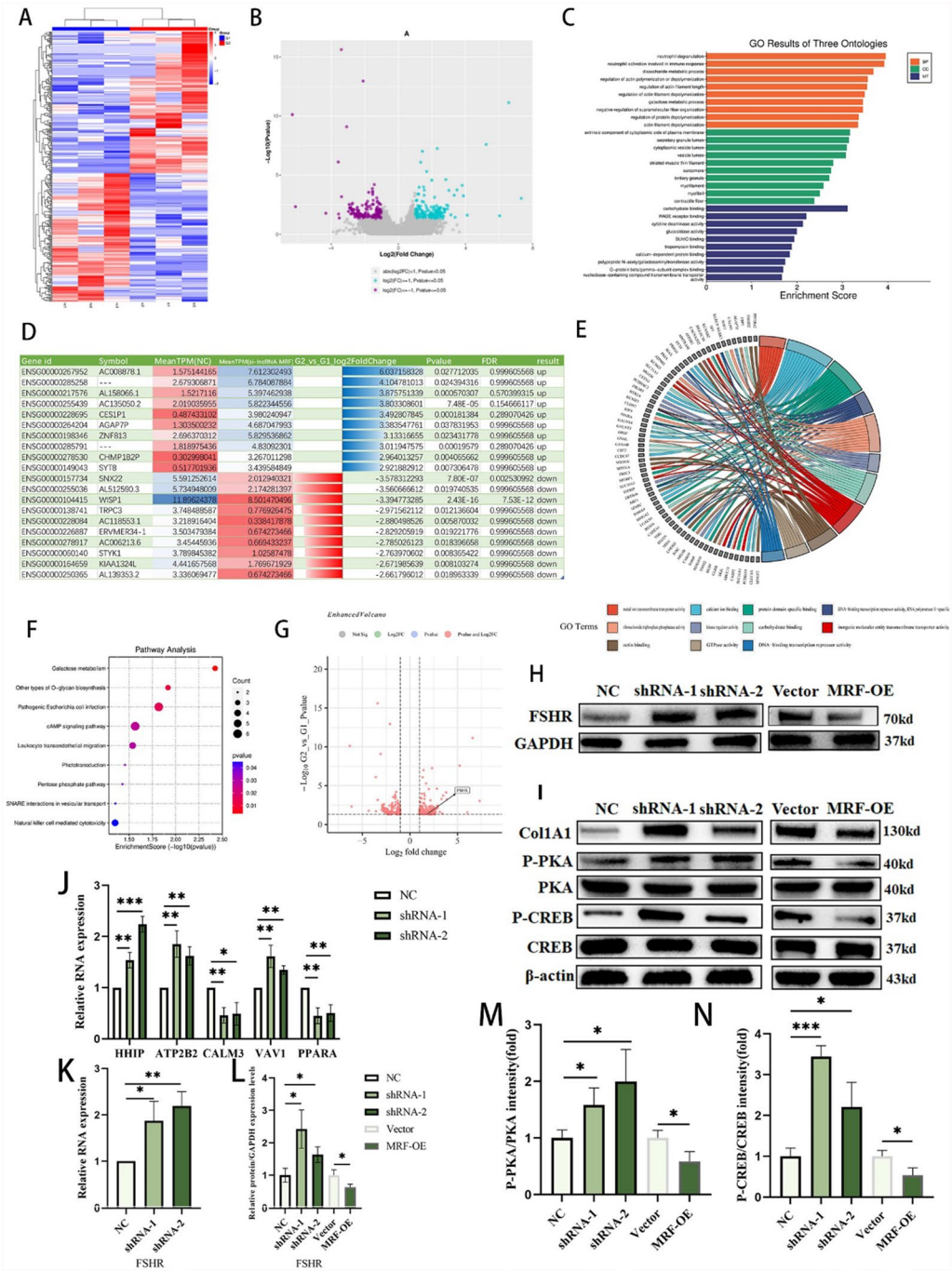

Fig. 4 (See legend on previous page.)

of both MRF and FSHR exhibited a marked reduction in the ratios of P-PKA/PKA and P-CREB/CREB (Fig. 5c, f), indicating that FSHR knockdown inhibits the activation of the cAMP-PKA-CREB signaling pathway induced by MRF knockdown. In addition, we ordered the cAMP/PKA/CREB signaling pathway inhibitor H-89 (a potent PKA inhibitor) and conducted further rescue experiments. CCK-8 assays demonstrated that, compared to the negative control group, the viability of BMSCs remained unaffected when exposed to H-89 at concentrations below 10 μM for a duration of 24 h (Fig. 5j). The results demonstrated that, compared to NC group, BMSCs treated with SI-MRF displayed an enhanced osteogenic phenotype. However, the addition of H-89

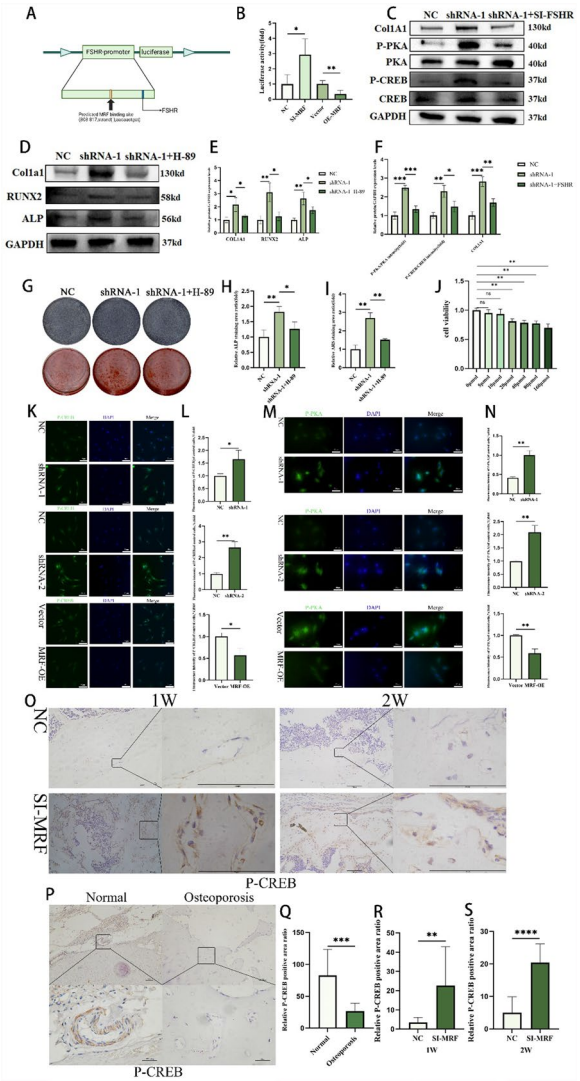

◀ **Fig. 5** The LncRNA MRF governs osteogenic differentiation via the FSHR-cAMP-PKA-CREB signaling pathway. **a** The pattern map lists the binding sites of lncRNA MRF in the FSHR promoter and the sequence of the predicted lncRNA MRF binding site. **b** Dual-luciferase assays on LncRNA MRF and the promoters of FSHR (n = 3). **c** Western blot showing changes in the expression of P-PKA/PKA, P-CREB/CREB after knocking down LncRNA MRF or knocking down LncRNA MRF and FSHR at the same time. **d** Western blot showing changes in the expression of osteogenic related proteins after knocking down LncRNA MRF or knocking down LncRNA MRF after using H-89. **e**, **f**Quantification of specific signal intensities. GAPDH was used as the loading control. Values are presented as mean ± standard deviation (SD) for three independent experiments (n = 3) (*$p < 0.05$, **$p < 0.01$, ***$p < 0.001$). **g** Treatment of BMSCs with SI-MRF and SI-MRF+H-89 during osteogenic differentiation followed by ARS/ALP staining. **h**, **i** Image J was used to analyze the positive area of ARS/ALP staining (n = 3). **j** viability of BMSCs cultured with 0 ~ 160μM H-89 for 24h (n = 3). **k**, **m** Immunofluorescence images (20 X) showing P-CREB, P-PKA staining of BMSCs treated shRNA-1, shRNA-2, and MRF overexpression plasmids and Osteogenic induction for three days. **l**, **n** Image J was used to analyze the Immunofluorescence intensity of P-CREB, P-PKA. The data are presented as the mean ± SD (n = 3) (*$p < 0.05$, **$p < 0.01$, ***$p < 0.001$). **o** Immunohistochemistry of P-CREB in local injection of negative controls siRNA group or lncRNA MRF knockdown siRNA group with 1w or 2w. **p** Immunohistochemistry of P-CREB in normal bone tissue and bone tissue of patients with osteoporosis. **q**, **r**, **s** The positive area ratio was evaluated by Image J (n = 3). The data are presented as the mean ± SD (*$p < 0.05$, **$p < 0.01$, ***$p < 0.001$). Full-length blots are presented in Supplementary material 1: Figures 25–34. The cropping position of the original image is marked in Supplementary material 1: documents 1

(10 μM) significantly decreased the levels of osteogenic marker proteins (Fig. 5d, e). Similarly, the enhancement of osteogenesis in BMSCs induced by SI-MRF was mitigated in the presence of H-89, as reflected by the corresponding reductions in ALP activity and Alizarin Red staining intensity (Fig. 5g, h, i). Additionally, immunofluorescence analyses of p-PKA and p-CREB corroborate these findings (Fig. 5k–n), with BMSCs treated with siRNA-MRF displaying a brighter fluorescence of p-PKA and p-CREB, compared to the negative control group. Immunohistological staining of p-CREB shows that tibial defects injected with lncRNA MRF knockdown siRNA present a greater number of p-CREB positive cells (Fig. 5o, r, s). Immunohistochemical staining for p-CREB confirmed a decrease in bone formation markers in osteoporosis patients (Fig. 5p, q). The result demonstrates that lncRNA MRF is also associated with the cAMP-PKA-CREB signaling pathway in human tissues. Overall, depletion of lncRNA MRF can activate the FSHR-cAMP-PKA-CREB signaling pathway, contributing to the osteogenic differentiation of BMSCs and enhancing their bone repair capabilities (Fig. 6).

Discussion

In conclusion, our study delved into the impact of lncRNA MRF on BMSCs' osteogenic differentiation and its activation of related pathways. Our results demonstrate that downregulation of lncRNA MRF significantly enhances ALP activity, osteogenic marker proteins, and mRNA expression. Additionally, this downregulation promotes the FSHR-cAMP-PKA-CREB signaling pathway, which plays a crucial role in the lncRNA MRF-mediated regulation of BMSCs osteogenic differentiation, thereby facilitating the osteogenic differentiation process. We suggest that lncRNA MRF exerts an inhibitory effect on osteogenesis primarily through the cAMP/PKA/CREB signaling pathway. Moreover, we validated the in vivo role of lncRNA MRF in osteogenesis and bone repair using a mouse tibial drilling model [12].

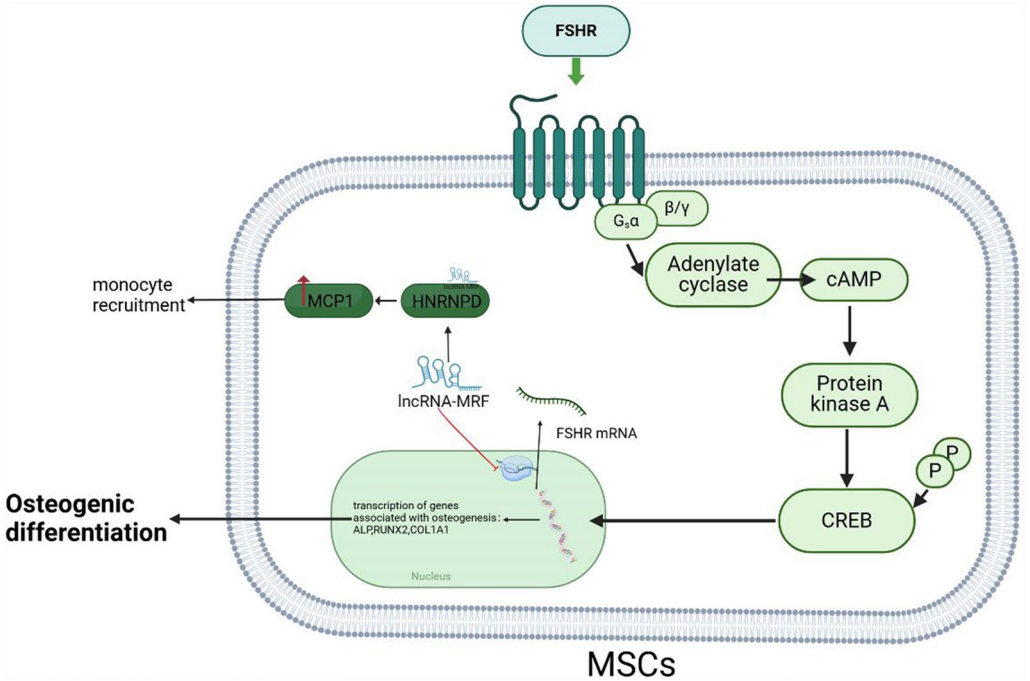

Fig. 6 Pattern diagram of the mechanism of action of LncRNA MRF in BMSCs. MRF modulates the cAMP/PKA/CREB signaling axis through FSHR, thereby adjusting the ossification differentiation of BMSCs. Our research suggests that MRF may a potential target for bone related disorders.

lncRNA were initially considered to be transcriptional remnants without biological significance. However, extensive research has gradually uncovered their crucial roles in various cellular processes [13]. Recent studies have confirmed that lncRNA play a significant role in the differentiation of BMSCs [14], with specific lncRNA identified as regulators of BMSCs' osteogenesis. BMSCs play a key role in differentiating into osteoblasts and adipocytes [4], while also exhibiting immunomodulatory functions. MSCs have strong immune regulatory ability and are widely used in clinical treatment. They exhibit bidirectional immune regulatory ability under different immune states, which can mobilize immune cells by secreting various cytokines and exhibit pro-inflammatory effects [15]. Additionally, MSCs can also inhibit the proliferation of pro-inflammatory cells and increase the number of anti-inflammatory cells such as anti-inflammatory macrophages. This is achieved through the chemokine-iNOS-IDO axis or the production of metabolites such as cytokines (TGF-β, IL-6) and prostaglandin E2 (PGE) [16]. The osteogenic differentiation process of MSCs involves multiple pathways, including the Wnt/β-catenin pathway, Bmp-Smad pathway, Hedgehog signaling, and the cAMP signaling pathway [17]. Understanding how MSCs regulate both immune responses and osteogenic differentiation is crucial for enhancing MSC-based therapies. However, the specific molecules that act as key regulators or switches in these processes are still unknown. Our research indicates that lncRNA MRF not only influences immune responses but also controls osteogenic differentiation. The knockdown of lncRNA MRF may suppress M1 macrophage polarization, enhance M2 macrophage polarization, and promote osteogenesis in MSCs. Therefore, lncRNA MRF is identified as a critical molecule that coordinates the immune and osteogenic processes in MSCs, serving as a central regulator in driving functional changes and biological behavior modifications in these cells.

lncRNA play a crucial role in modulating cellular activities through various mechanisms, such as acting as sponges, signals, and guides, as well as interacting with DNA, RNA, and proteins. In the context of bone differentiation, lncRNA function as competing endogenous RNAs (ceRNAs) and also interact with RNA-binding proteins (RBP), RNA duplexes, and activate signaling pathways like BMP4. For instance, Liu et al. [18] studied the lncRNA GATA2AS, which is expressed in human erythrocytes. They discovered that it is transcribed in opposition to the erythroid transcription regulator GATA2, modulating erythroid differentiation through influencing the binding of transcription factor GATA2. Similarly, Zhang et al. [19] observed high expression of the lncRNA Snhg7 in cardiomyocytes with myocardial hypertrophy. Their research revealed that Snhg7 induced ferroptosis

by interacting with the T-box transcription factor 5 and glutaminase 2, inhibiting Snhg7 led to a decrease in Tbx5 and GLS2 expression, thereby reducing iron-dependent cell death and impacting the progression of myocardial hypertrophy. Furthermore, Liu et al. [20] examined the function of the LINC01594 lncRNA in colon cancer cells and found that it acted as a scaffold for DNMT1, resulting in increased methylation levels of the CELF6 promoter. Additionally, LINC01594 competitively bound the transcription factor P53, reducing CELF6 expression and facilitating colon cancer metastasis. In our findings, Following the downregulation of lncRNA MRF, an increase was observed in both mRNA and protein levels of FSHR. It is postulated that lncRNA MRF may function through RNA-RNA interactions, potentially transcriptionally mediated. Based on this, we conducted dual-luciferase assays, which showed that knocking down lncRNA-MRF significantly increased the transcriptional activity of FSHR. This finding suggests that MRF may inhibit the transcription of FSHR. To gain more conclusive insights into how lncRNA MRF influences downstream molecules, further investigations such as bioinformatics predictive analyses and RNA pull-down experiments are necessary to explore RNA-RNA interactions in depth. Additionally, the use of activators and inhibitors in the cAMP-PKA-CREB pathway is essential for refining recovery experiments and elucidating the specific mechanisms by which MRF modulates the FSHR-cAMP-PKA-CREB pathway. In our recovery experiment, we used H-89, an effective PKA inhibitor, to block the activation of the cAMP signaling pathway. This inhibition mitigated the osteogenic enhancement effect in BMSCs caused by the knockdown of lncRNA MRF, indicating that lncRNA MRF/FSHR can influence the cAMP/PKA/CREB signaling pathway, thereby regulating bone differentiation. Moving forward, we plan to use an activator of the cAMP signaling pathway for further verification.

Cyclic Adenosine Monophosphate (cAMP) is a widely distributed molecule in cells, serving as a critical secondary messenger for various hormones and neurotransmitters. It regulates key biological processes, including cellular metabolism, gene expression, growth, differentiation, and apoptosis [21]. cAMP can be produced through G-protein activation of Adenylyl Cyclase (ACs) or by G-protein independent soluble Adenylate Cyclase (sAC) [22]. As a G protein-coupled receptor, the Follicle Stimulating Hormone Receptor (FSHR) is reported to regulate cellular activities by influencing downstream cAMP signaling pathways. Our RNA-seq samples involve three age groups, which helps us understand the universality of gene expression changes in BMSCs caused by MRF knockout in individuals of different ages [23], while showing that the knockdown of lncRNA MRF leads to a significant increase in FSHR expression. Therefore, we propose the hypothesis that lncRNA MRF regulates the cAMP signaling pathway via FSHR and have conducted experiments to validate this hypothesis. In our follow-up experiments, simultaneously knocking down both lncRNA-MRF and FSHR in BMSCs led to a decrease in the phosphorylation levels of PKA and CREB, compared to knocking down lncRNA-MRF alone. Knockdown of FSHR inhibited activation of the cAMP signaling pathway, further supporting our hypothesis. The effects of cAMP are primarily mediated through the activation of Protein Kinase A (PKA), leading to the phosphorylation of cAMP-responsive element binding protein (CREB) for regulatory purposes. Downstream molecules like Raf, Bad, and GSK3 can also be influenced. Previous research has indicated that lncRNA have the ability to modulate the cAMP-PKA-CREB signaling pathway [24]. For example, Chen et al. [25] demonstrated that lncRNA-M2 can interact with PKA in M2 macrophages, facilitating M2 macrophage differentiation through the PKA/CREB pathway. In our study on BMSCs, we have uncovered for the first time the involvement of lncRNA in the regulation of the FSHR-cAMP-PKA-CREB pathway. The cAMP signaling pathway is crucial for regulating osteogenic differentiation and bone formation. Parathyroid hormone (PTH) is the only FDA-approved anabolic medication for osteoporosis in the USA [26]. Numerous studies have shown a link between PTH-stimulated G-protein-coupled receptor PTH1R-specific induction of cAMP/PKA pathway activation and PTH-induced osteogenic differentiation. Further research confirms the significance of the cAMP/PKA pathway in osteogenesis. Kim et al. [27] utilized cAMP/PKA/CREB pathway activators to stimulate BMSCs, demonstrating its ability to promote human BMSCs osteoblast differentiation and enhance bone formation in ovariectomized mice. Activation of cAMP pathways in primary aortic medial cells has been shown to promote mineralization and vascular calcification by enhancing osteoblast-like differentiation, which aligns with the findings of our own research [28].

Numerous recent studies have focused on the use of lncRNA in treating human skeletal diseases, with BMSCs emerging as the preferred gene therapy vehicle due to their low immunogenicity [29]. These BMSCs are genetically modified and then administered either systemically or locally to address conditions like osteoporosis, osteoarthritis, and degenerative disc diseases. Natália de Melo Ocarino et al. [30] conducted a study where they injected 750,000 BMMSCs from healthy rats into the femurs of osteoporotic rats, resulting in increased bone differentiation and mass. This demonstrated the

effectiveness of BMSCs injections for osteoporosis. Another study by Li [31] explored the overexpression of BMMSCs-related lncRNA Bmncr in BMSCs and found it could help mitigate age-related bone loss in mouse models. Using an adeno-associated virus vector (rAAV9-Sp7-Taz-GFP) coding for Taz, the study delivered it into the osteoprogenitor cells of Bmncr-KO mice through intra-osseous injections, showing that the overexpression of Taz partially reversed the premature aging of bones in these mice. Similarly, Mahasen Al-Najar's [32] research involving the injection of BMSCs into knee osteoarthritic patients demonstrated safety and significant improvement during the two-year follow-up. Our studies have demonstrated that the direct injection of si-lncRNA into the perforated sections of mice bones effectively enhances bone formation at the site of injury. This method is comparatively easier to implement than injecting BMSCs, and the enhanced bone formation at the site of drilled bone is strikingly evident. Previous research has also reported success via direct in vivo siRNA injections to mitigate disease progression in mice; for instance, a study by Gong [33] found that knee arthroscopic injections of YAP siRNA resulted in an alleviation of the mice's osteoarthritis symptoms by reducing abnormal subchondral bone formation and inhibiting the progress of osteoarthritis. However, directly injecting si-lncRNA into bone tissue may pose potential risks, including local immune responses, direct toxicity to surrounding cells, unintended targeting of other mRNAs with similar sequences, and local irritation symptoms such as pain, swelling, and redness. Additionally, the effects of siRNA are typically transient, necessitating repeated injections over an extended period to maintain efficacy, which further amplifies these risks. Therefore, it is crucial to thoroughly assess these risks before designing and implementing experiments. This includes optimizing the dosage and frequency of administration and focusing on developing delivery systems that specifically target BMSCs. Existing delivery strategies include nanospheres, liposomes, adenoviruses/lentiviruses, hydrogel scaffolds, and monoclonal antibody/antigen-binding systems. Huang et al. [34] developed bone-targeting liposomes that effectively encapsulate compounds, demonstrating specific targeting of bone tissue. In in vivo experiments, this delivery system enhanced bone formation in ovariectomized mice, indicating that the Asp8-liposome effectively carries osteogenic compounds, thereby enhancing therapeutic outcomes against osteoporosis caused by estrogen depletion. In future clinical translation processes, emphasis should be placed on designing material systems for the targeted delivery of MRF to BMSCs. This approach aims to minimize injection-related damage and improve the specificity and efficacy of MRF silencing. This body of research supports our findings. As an in-depth investigation into the role of lncRNA in tissue engineering continues, lncRNA and their target genes hold potential as therapeutic targets for bone-related ailments.

The study enhances our comprehension of the inhibitory function of lncRNA MRF in osteogenesis, providing a molecular basis for potential therapies targeting osteoporosis. From a clinical perspective, the investigated lncRNA MRF could serve as a promising therapeutic target for promoting bone differentiation. Knocking down lncRNA MRF with siRNA significantly enhances osteogenesis both in vitro and in vivo, as well as bone formation at tibial defect sites. However, this study has certain limitations. Firstly, the current in vivo experiments could be further optimized by using a targeted delivery system for BMSCs, which would help clarify the role of MRF in vivo while minimizing interference from its effects on other cell types. Secondly, developing an osteoporosis mouse model is necessary for more in-depth in vivo studies, to better understand the mechanisms by which lncRNA MRF functions in the context of osteoporosis. Thirdly, while osteoblasts and osteoclasts are indeed critical effector cells in bone metabolism, osteocytes play a fundamental role in maintaining bone homeostasis by integrating mechanical, biochemical, and hormonal signals. Investigating the effects of MRF on osteocytes and osteoclasts, as well as its potential specific mechanisms, will be a key focus of our future experimental direction.

Conclusion

Our research explored the impact of lncRNA MRF on osteogenic differentiation of BMSCs both in vitro and in vivo. We introduced the novel concept that lncRNA MRF modulates BMSCs osteogenesis via the FSHR-cAMP-PKA-CREB signaling pathway. These findings enhance our comprehension of the regulatory mechanisms involved in BMSCs osteogenesis and present potential therapeutic targets for clinical interventions. However, our study is not without limitations. Specifically, the exact mechanisms by which lncRNA MRF influences osteoporosis progression remain elusive, and the efficacy of lncRNA MRF inhibitors in clinical settings has yet to be established. These are areas that warrant further investigation.

Resource availability

Lead contact.

Further information and requests for resources and reagents should be directed to and will be fulfilled by the lead contact by the lead contact, Lin Huang (huangl5@mail.sysu.edu.cn).

Supplementary Information

The online version contains supplementary material available at https://doi.org/10.1186/s13287-025-04291-9.

Supplementary material 1

Acknowledgements
This work was supported by Natural Science Foundation of Guangdong Province (2021A1515111013, 2022A1515012305), Guangzhou Science and technology planning project (202201010881).

Author contributions
QN, ML, LH designed the study; QN, ML, ZL, EC, HL performed experiments and YL, YL, YC analyzed the data; QN, ML, LH wrote this manuscript.

Funding
This work was supported by Natural Science Foundation of Guangdong Province (2021A1515111013, 2022A1515012305), Guangzhou Science and Technology Planning Project (202201010881).

Availability of data and materials
RNA-seq data generated in this study are available at the Geo database (GEO: GSE272041). Code for differential expression analysis is available at www.metascape.org [35].

Materials availability
This study did not generate new unique reagents.

Declarations
The authors declare that they have not used Artificial Intelligence in this study.

Ethics approval and consent to participate
The collection of human tissue.
(1) Title of the approved project;
靶向FSHR的LncRNA MRF通过cAMP-PKA-CREB信号通路参与骨髓间充质干细胞成骨分化及骨缺损修复.
(2) Name of the institutional approval committee or unit;
Medical Ethics Committee (Research) of Sun Yat-Sen Memorial Hospital, Sun Yat-Sen University.
(3) Approval number;
Ethical approval number: SYSKY-2024–379-01.
(4) Date of approval.
Approved on April 16, 2024.
The animal experiments.
(1) Title of the approved project;
LncRNA MRF 通过调控 BMP6蛋白降解抑制 MSCs 成骨分化在骨质疏松症中的机制研究.
(2) Name of the institutional approval committee or unit;
The animal experiments conducted at Sun Yat-Sen University were approved by the SYSU Institutional Animal Care and Use Committee.
(3) Approval number;
Ethical approval number: SYSU-IACUC-2024-001134.
(4) Date of approval.
Approved on March 24, 2024.
The study was conducted in accordance with the Declaration of Helsinki. All participants in the study have obtained informed consent.

Consent for publication
All authors confirm their consent for publication.

Competing interests
The authors declare no competing interests.

Received: 24 July 2024 Accepted: 24 March 2025
Published online: 23 April 2025

References

1. Wu S, Ohba S, Matsushita Y. Single-cell RNA-sequencing reveals the skeletal cellular dynamics in bone repair and osteoporosis. Int J Mol Sci. 2023;24:9814.
2. Ju C, Liu R, Zhang YW, Zhang Y, Zhou R, Sun J, et al. Mesenchymal stem cell-associated lncRNA in osteogenic differentiation. Biomed Pharmacother. 2019;115: 108912.
3. Zhang R, Li J, Li G, Jin F, Wang Z, Yue R, et al. LncRNA Nron regulates osteoclastogenesis during orthodontic bone resorption. Int J Oral Sci. 2020;12:14.
4. Huang Y, Wu Q, Tam P. Immunomodulatory mechanisms of mesenchymal stem cells and their potential clinical applications. Int J Mol Sci. 2022;23:10023.
5. Lin J, Xie Z, Zhang Z, Li M, Ye G, Yu W, et al. LncRNA MRF drives the regulatory function on monocyte recruitment and polarization through HNRNPD-MCP1 axis in mesenchymal stem cells. J Biomed Sci. 2022;29:73.
6. Tye CE, Ghule PN, Gordon J, Kabala FS, Page NA, Falcone MM, et al. Lnc-MIR181A1HG is a novel chromatin-bound epigenetic suppressor of early stage osteogenic lineage commitment. Sci Rep. 2022;12:7770.
7. Wang X, Yang J, Guo G, Feng R, Chen K, Liao Y, et al. Novel lncRNA-IUR suppresses Bcr-Abl-induced tumorigenesis through regulation of STAT5-CD71 pathway. Mol Cancer. 2019;18:84.
8. Ding Y, Wei J, Hettinghouse A, Li G, Li X, Einhorn TA, et al. Progranulin promotes bone fracture healing via TNFR pathways in mice with type 2 diabetes mellitus. Ann N Y Acad Sci. 2021;1490:77–89.
9. Koblenzer M, Weiler M, Fragoulis A, Rutten S, Pufe T, Jahr H. Physiological mineralization during in vitro osteogenesis in a biomimetic spheroid culture model. Cells-Basel. 2022;11:2702.
10. Moradifard S, Hoseinbeyki M, Emam MM, Parchiniparchin F, Ebrahimi-Rad M. Association of the Sp1 binding site and -1997 promoter variations in COL1A1 with osteoporosis risk: the application of meta-analysis and bioinformatics approaches offers a new perspective for future research. Mutat Res Rev Mutat Res. 2020;786: 108339.
11. Tang D, Chen M, Huang X, Zhang G, Zeng L, Zhang G, et al. SRplot: a free online platform for data visualization and graphing. PLoS ONE. 2023;18: e294236.
12. Tanaka K, Tanaka S, Sakai A, Ninomiya T, Arai Y, Nakamura T. Deficiency of vitamin A delays bone healing process in association with reduced BMP2 expression after drill-hole injury in mice. Bone. 2010;47:1006–12.
13. Jankowski M, Farzaneh M, Ghaedrahmati F, Shirvaliloo M, Moalemnia A, Kulus M, et al. Unveiling mesenchymal stem cells' regenerative potential in clinical applications: insights in miRNA and lncRNA implications. Cells-Basel. 2023;12:2559.
14. Xie ZY, Wang P, Wu YF, Shen HY. Long non-coding RNA: The functional regulator of mesenchymal stem cells. World J Stem Cells. 2019;11:167–79.
15. Wang Y, Fang J, Liu B, Shao C, Shi Y. Reciprocal regulation of mesenchymal stem cells and immune responses. Cell Stem Cell. 2022;29:1515–30.
16. Shi Y, Wang Y, Li Q, Liu K, Hou J, Shao C, et al. Immunoregulatory mechanisms of mesenchymal stem and stromal cells in inflammatory diseases. Nat Rev Nephrol. 2018;14:493–507.
17. Liang B, Burley G, Lin S, Shi YC. Osteoporosis pathogenesis and treatment: existing and emerging avenues. Cell Mol Biol Lett. 2022;27:72.
18. Liu G, Kim J, Nguyen N, Zhou L, Dean A. Long noncoding RNA GATA2AS influences human erythropoiesis by transcription factor and chromatin landscape modulation. Blood. 2024;143:2300–13.
19. Zhang Q, Song C, Zhang M, Liu Y, Wang L, Xie Y, et al. Super-enhancer-driven lncRNA Snhg7 aggravates cardiac hypertrophy via Tbx5/GLS2/ferroptosis axis. Eur J Pharmacol. 2023;953: 175822.
20. Liu B, Song A, Gui P, Wang J, Pan Y, Li C, et al. Long noncoding RNA LINC01594 inhibits the CELF6-mediated splicing of oncogenic CD44 variants to promote colorectal cancer metastasis. Cell Death Dis. 2023;14:427.
21. Zaccolo M, Zerio A, Lobo MJ. Subcellular organization of the cAMP signaling pathway. Pharmacol Rev. 2021;73:278–309.
22. Chuang SC, Chen CH, Chou YS, Ho ML, Chang JK. G protein-coupled estrogen receptor mediates cell proliferation through the cAMP/PKA/CREB pathway in murine bone marrow mesenchymal stem cells. Int J Mol Sci. 2020;21:6490.
23. Cui H, Han G, Sun B, Fang X, Dai X, Zhou S, et al. Activating PIK3CA mutation promotes osteogenesis of bone marrow mesenchymal stem cells in macrodactyly. Cell Death Dis. 2020;11:505.

24. Cui X, Xu Y, Zhu H, Wang L, Zhou J. Long noncoding RNA NONHSAG045500 regulates serotonin transporter to ameliorate depressive-like behavior via the cAMP-PKA-CREB signaling pathway in a model of perinatal depression. J Matern Fetal Neonatal Med. 2023;36:2183468.
25. Chen Y, Li H, Ding T, Li J, Zhang Y, Wang J, et al. Lnc-M2 controls M2 macrophage differentiation via the PKA/CREB pathway. Mol Immunol. 2020;124:142–52.
26. Chen T, Wang Y, Hao Z, Hu Y, Li J. Parathyroid hormone and its related peptides in bone metabolism. Biochem Pharmacol. 2021;192: 114669.
27. Kim JM, Choi JS, Kim YH, Jin SH, Lim S, Jang HJ, et al. An activator of the cAMP/PKA/CREB pathway promotes osteogenesis from human mesenchymal stem cells. J Cell Physiol. 2013;228:617–26.
28. Tintut Y, Parhami F, Bostrom K, Jackson SM, Demer LL. cAMP stimulates osteoblast-like differentiation of calcifying vascular cells. Potential signaling pathway for vascular calcification. J Biol Chem. 1998; 273: 7547–53.
29. Jacobs SA, Roobrouck VD, Verfaillie CM, Van Gool SW. Immunological characteristics of human mesenchymal stem cells and multipotent adult progenitor cells. Immunol Cell Biol. 2013;91:32–9.
30. Ocarino NM, Boeloni JN, Jorgetti V, Gomes DA, Goes AM, Serakides R. Intra-bone marrow injection of mesenchymal stem cells improves the femur bone mass of osteoporotic female rats. Connect Tissue Res. 2010;51:426–33.
31. Li CJ, Xiao Y, Yang M, Su T, Sun X, Guo Q, et al. Long noncoding RNA Bmncr regulates mesenchymal stem cell fate during skeletal aging. J Clin Invest. 2018;128:5251–66.
32. Al-Najar M, Khalil H, Al-Ajlouni J, Al-Antary E, Hamdan M, Rahmeh R, et al. Intra-articular injection of expanded autologous bone marrow mesenchymal cells in moderate and severe knee osteoarthritis is safe: a phase I/II study. J Orthop Surg Res. 2017;12:190.
33. Gong Y, Li SJ, Liu R, Zhan JF, Tan C, Fang YF, et al. Inhibition of YAP with siRNA prevents cartilage degradation and ameliorates osteoarthritis development. J Mol Med (Berl). 2019;97:103–14.
34. Huang L, Wang X, Cao H, Li L, Chow DH, Tian L, et al. A bone-targeting delivery system carrying osteogenic phytomolecule icaritin prevents osteoporosis in mice. Biomaterials. 2018;182:58–71.
35. Zhou Y, Zhou B, Pache L, Chang M, Khodabakhshi AH, Tanaseichuk O, et al. Metascape provides a biologist-oriented resource for the analysis of systems-level datasets. Nat Commun. 2019;10:1523.

Publisher's Note